

# Measurements of $t$ -channel single top-quark production cross sections at $\sqrt{s} = 7$ TeV with the ATLAS detector

Dominic Hirschtbühl

On behalf of the ATLAS Collaboration

Gausstr. 20, 42119 Wuppertal, Germany

E-mail: hirsch@physik.uni-wuppertal.de

**Abstract.** This article presents measurements of the  $t$ -channel single top-quark ( $t$ ) and top-antiquark ( $\bar{t}$ ) total production cross sections  $\sigma(tq)$  and  $\sigma(\bar{t}q)$ , their ratio  $R_t = \sigma(tq)/\sigma(\bar{t}q)$ . Differential cross sections for the  $\sigma(tq)$  and  $\sigma(\bar{t}q)$  processes are measured as a function of the transverse momentum and the absolute value of the rapidity of ( $t$ ) and ( $\bar{t}$ ), respectively. The analysed data set was recorded with the ATLAS detector and corresponds to an integrated luminosity of  $4.59 \text{ fb}^{-1}$ . The cross sections are measured by performing a binned maximum-likelihood fit to the output distributions of neural networks. The resulting measurements are  $\sigma(tq) = 46 \pm 6 \text{ pb}$ ,  $\sigma(\bar{t}q) = 23 \pm 4 \text{ pb}$ ,  $R_t = 2.04 \pm 0.18$ , consistent with the Standard Model expectation.

## 1. Introduction

In proton–proton ( $pp$ ) collisions at the LHC, top quarks are produced at unprecedented rates. Single top-quark production is described by three subprocesses that are distinguished by the virtuality of the exchanged  $W$  boson. The dominant process is the  $t$ -channel exchange. A light quark from one of the colliding protons interacts with a  $b$ -quark from another proton by exchanging a virtual  $W$  boson ( $W^*$ ). Since the  $u$ -quark density of the proton is about twice as high as the  $d$ -quark density, the production cross section of single top quarks  $\sigma(tq)$  is expected to be about twice as high as the cross section of top-antiquark production  $\sigma(\bar{t}q)$ . In  $pp$  collisions at  $\sqrt{s} = 7$  TeV, the total inclusive cross sections of top-quark and top-antiquark production in the  $t$ -channel are predicted to be  $\sigma(tq) = 41.9_{-0.9}^{+1.8} \text{ pb}$ ,  $\sigma(\bar{t}q) = 22.7_{-1.0}^{+0.9} \text{ pb}$  with approximate next-to-next-to-leading-order (NNLO) precision [1].

## 2. Event selection and background estimation

The analysis described in this article [2] uses  $pp$  LHC collision data collected at a center-of-mass energy of 7 TeV with the ATLAS detector [3]. Stringent detector and data quality requirements are applied, resulting in a data set corresponding to an integrated luminosity of  $4.59 \pm 0.08 \text{ fb}^{-1}$ . The event selection requires exactly one charged isolated lepton ( $e$  or  $\mu$ ), exactly two or three jets, and  $E_{\text{T}}^{\text{miss}} > 30 \text{ GeV}$ . Electron candidates are selected from energy deposits in the LAr electromagnetic calorimeter matched to tracks and are required to have  $E_{\text{T}} > 25 \text{ GeV}$  and  $|\eta| < 2.47$ . Muon candidates are reconstructed by combining track segments found in the inner

detector and the muon spectrometer. Only candidates that have  $p_T > 25$  GeV and  $|\eta| < 2.5$  are considered. Jets are reconstructed using the anti- $k_t$  algorithm with a radius parameter of 0.4 and have to have  $p_T > 30$  GeV and  $|\eta| < 4.5$ . Jets in the endcap/forward-calorimeter transition region, corresponding to  $2.75 < |\eta| < 3.5$ , must have  $p_T > 35$  GeV. At least one of the jets must be  $b$ -tagged. Since the multijet background is difficult to model precisely, its contribution is reduced by  $m_T(\ell E_T^{\text{miss}}) = \sqrt{2p_T(\ell) \cdot E_T^{\text{miss}} [1 - \cos(\Delta\phi(\ell, E_T^{\text{miss}}))]} > 30$  GeV and by requiring  $\Delta\phi(j_1, \ell) p_T(\ell) > 40 \text{ GeV} \cdot \left(1 - \frac{\pi - |\Delta\phi(j_1, \ell)|}{\pi - 1}\right)$ , where  $j_1$  denotes the leading jet. The  $W$ +jets background is initially normalized to the theoretical prediction and then subsequently determined simultaneously both in the context of the multijet background estimation and as part of the extraction of the signal cross section. The estimated number of events of the theoretically well know ( $t\bar{t}$ ,  $Wt$ ,  $s$ -channel single top-quark production) or small processes ( $WW$ ,  $WZ$  and  $ZZ$ ,  $Z$ +jets background) are calculated using the theoretical prediction. Data driven techniques are used to derive the multijet background. In the electron channel the jet-lepton method is used. There an electron-like jet is selected with special requirements and redefined as a lepton. A binned maximum-likelihood fit to observed data in the  $E_T^{\text{miss}}$  distribution, omitting the  $E_T^{\text{miss}}$  requirement in the selection, to obtain the normalization, as shown in Figure 1.

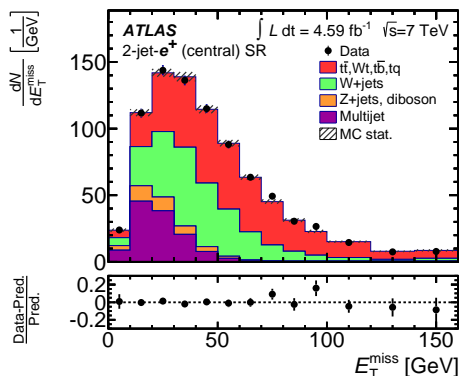


**Figure 1.**  $E_T^{\text{miss}}$  distributions in the signal region (SR) for the 2-jet- $e^+$  channel for central electrons. The distributions are normalized to the result of a binned maximum-likelihood fit. The relative difference between the observed and expected number of events in each bin is shown in the lower panels.

In the muon channel, the matrix method is used to obtain both the normalization and shape of the multijet background. The method estimates the number of multijet background events in the signal region based on loose and tight lepton isolation definitions, the latter selection being a subset of the former.

### 3. Signal extraction

To separate  $t$ -channel single top-quark signal events from background events, several kinematic variables are combined to form powerful discriminants by employing neural networks. The NeuroBayes [4] tool is used for preprocessing the input variables and for the training of the NNs. A large number of potential input variables were studied and the correct modeling of the variables is checked in a control region. In Figure 2, the probability densities of the resulting NN discriminants in one channel for the signal and the most important backgrounds is shown.

The cross sections  $\sigma(tq)$  and  $\sigma(\bar{t}q)$  are extracted by performing a binned maximum-likelihood fit to the NN discriminant distributions in the 2-jet- $\ell^+$ , 2-jet- $\ell^-$ , 3-jet- $\ell^+$ -1-tag, and 3-jet- $\ell^-$ -1-tag channels and to the event yield in the 3-jet-2-tag channel, treating  $t$ -channel top-quark and  $t$ -channel top-antiquark production as independent processes. The cross-section ratio is subsequently computed as  $R_t = \sigma(tq)/\sigma(\bar{t}q)$ . In Figure 3 the observed NN discriminant distribution in the 2-jet- $\ell^+$  channel is shown compared to the compound model of signal and background normalized to the fit results.

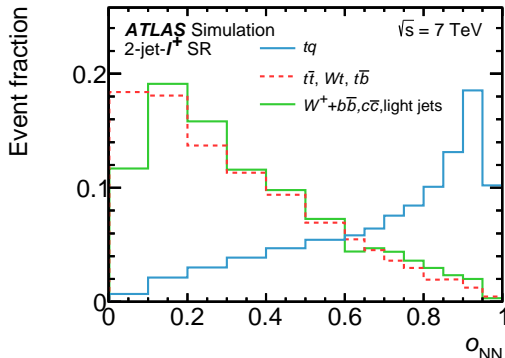


**Figure 2.** Probability densities of the NN discriminants in the 2-jet- $\ell^+$  channel in the signal region (SR). The distributions are normalized to unit area.

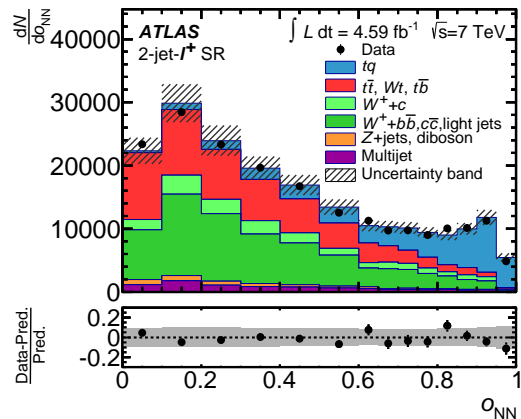


**Figure 3.** Neural network discriminant distributions normalized to the fit result in the 2-jet- $\ell^+$  channel. The relative difference between the observed and expected number of events is shown in the lower panels.

#### 4. Systematic uncertainties

Systematic uncertainties are assigned to account for detector calibration and resolution uncertainties, as well as the uncertainties of theoretical predictions. Uncertainties on the reconstruction and energy calibration of jets, electrons and muons are propagated through the entire analysis. Systematic uncertainties arising from the modeling of the single top-quark signal, the  $t\bar{t}$  background, and the  $W$ +jets background are taken into account as well as uncertainties related to the PDFs.

The systematic uncertainties on the individual top-quark and top-antiquark cross-section measurements and their ratio are determined using pseudo-experiments that account for variations of the signal acceptance, the background rates, and the shape of the NN discriminant. The correlations between the different channels and the physics processes are fully accounted for. The dominant systematic uncertainty on the cross sections is the JES  $\eta$ -intercalibration uncertainty.

#### 5. Total cross-section measurements

After performing the binned maximum-likelihood fit and estimating the total uncertainty the results are:

$$\begin{aligned}\sigma(tq) &= 46 \pm 1 \text{ (stat.)} \pm 6 \text{ (syst.) pb} &= 46 \pm 6 \text{ pb,} \\ \sigma(\bar{t}q) &= 23 \pm 1 \text{ (stat.)} \pm 3 \text{ (syst.) pb} &= 23 \pm 4 \text{ pb} \quad \text{and} \\ R_t &= 2.04 \pm 0.13 \text{ (stat.)} \pm 0.12 \text{ (syst.)} = 2.04 \pm 0.18.\end{aligned}$$

Figure 4 compares the measured values of  $R_t$  to NLO predictions from MCFM [5] and Hathor [6] using different PDF sets.

#### 6. Differential cross-section measurements

A high-purity region (HPR) is defined to measure the differential cross sections in the 2-jet- $\ell^+$  and 2-jet- $\ell^-$  channels, by requiring the NN discriminant to be larger than 0.8. In the 2-jet- $\ell^+$  HPR the signal contribution is twice as large as the background contribution, while it is approximately the same size in the 2-jet- $\ell^-$  HPR. Differential cross sections are measured as a function of the  $p_T$  and  $|y|$  of  $t$  and  $\bar{t}$ . The binning of the differential cross sections is chosen

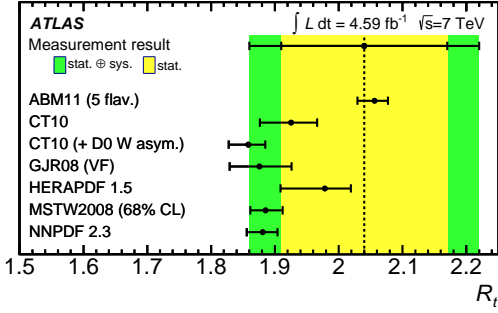


**Figure 4.** Comparison between observed and predicted values of  $R_t$ . The predictions are calculated at NLO precision in the five-flavor scheme and given for different NLO PDF sets and the uncertainty includes the uncertainty on the renormalization and factorization scales, the combined internal PDF and  $\alpha_s$  uncertainty.

based on the experimental resolution of the  $p_T$  and  $|y|$  distributions as well as the data statistical uncertainty. The measured distributions are distorted by detector effects and acceptance effects therefore the observed distributions are unfolded to the four-momenta of the top quarks before the decay and after QCD radiation. A migration matrix is built by relating the variables at the reconstruction and at the parton level using the signal simulation and the selection efficiency of each variable is defined as the ratio of the parton-level yield before and after selection. A graphical representation of the unfolded top quark  $p_T$  distribution is shown in Figure 5 and for the rapidity in Figure 6. Both distributions are compared to NLO predictions from MCFM using the MSTW2008 PDF set. For of the normalized differential cross sections many systematic uncertainties cancel and thus the measurement is dominated by the statistical uncertainty and the uncertainty due to the Monte Carlo sample size.

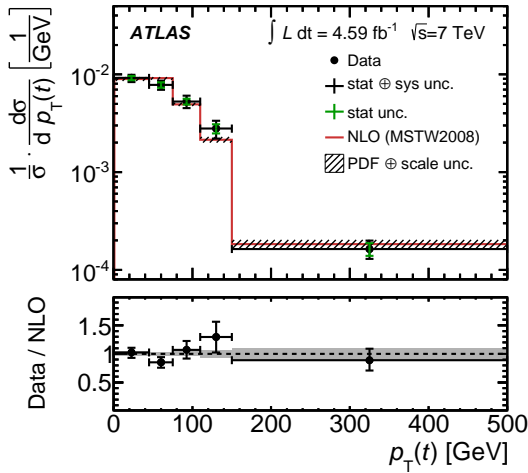


**Figure 5.** Differential cross section as a function of  $p_T(t)$ .

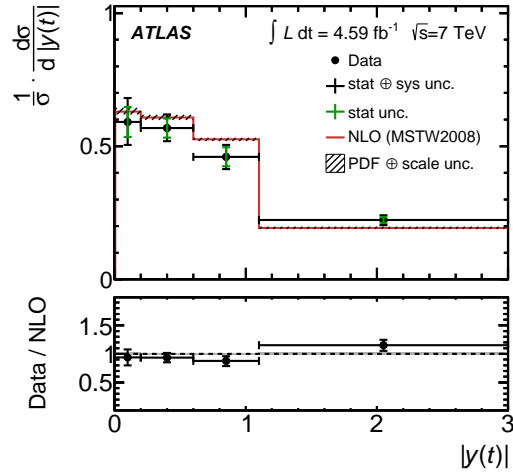


**Figure 6.** Differential cross section as a function of  $y(t)$ .

## References

- [1] Kidonakis N 2011 *Phys. Rev. D* **83** 091503
- [2] ATLAS Collaboration 2014 (*Preprint* 1406.7844)
- [3] ATLAS Collaboration 2008 *JINST* **3** S08003
- [4] Feindt M and Kerzel U 2006 *Nucl. Instrum. Meth. A* **559** 190–194
- [5] Campbell J M, Frederix R, Maltoni F and Tramontano F 2009 *Phys. Rev. Lett.* **102** 182003
- [6] Kant P, Kind O, Kintscher T, Lohse T, Martini T, Moelbitz S, Rieck P and Uwer P 2014 (*Preprint* 1406.4403)